Journal of Ceramic Processing Research. Vol. 25, No. 2, pp. 151~158 (2024)
(Received 23 March 2023, Received in revised form 12 December 2023, Accepted 15 December 2023)
https://doi.org/10.36410/jcpr.2024.25.2.151

J O U R N A L O F
Ceramic Processing Research

Application of Taguchi based entropy weighted TOPSIS method for AZ 91D magnesium alloy friction stir welded joints with cerium addition at interface

K. Rajesh Kumar[a,*], Kiran Kumar Dama[b] and Vaddi Venkatasatyanarayana[c]
[a]*Research Scholar, Department of Mechanical Engineering, Koneru Lakshmaiah Education Foundation, Vaddeswaram, Andhra Pradesh, India*
[b]*Associate Professor, Department of Mechanical Engineering, Koneru Lakshmaiah Education Foundation, Vaddeswaram, Andhra Pradesh, India*
[c]*Professor, Department of Mechanical Engineering, Vidya Jyothi Institute of Technology, Hyderabad, India*

Purpose: The alloy needed for friction stir welding must be able to fracture during the solidification and joining processes. To overcome some of these problems solid state welding processes have been identified as alternative and Friction stir welding process (FSW) is one found to be more prominent to join simple to complex geometries. In this investigation, FSW of AZ91D magnesium alloy is undertaken with cerium microparticles embedded into the weldment in order to produce a metal matrix composite at the stir zone. Design/methodology/Approach: AZ 91D magnesium alloy materials are friction welded by keeping cerium powder between the plates to be joined before the joining process. Magnesium alloy is the type of raw material that used for various mechanical industries since it has the good thermal conductivity, and lightweight. The solid state joining process employs friction stir welding. The commercial Mg alloys consists of various elements like Al, Mn, and Zn. Taguchi L9 OA is employed for the experimentation and three factors namely rotational speed, Feed of Tool and tilt angle of tool are used. The results are analyzed with entropy weighted TOPSIS method. The overall outcome is predicted and confirmation test results are compared with it.

Keywords: FSW process, AZ 91D Magnesium alloy, Cerium powder, Taguchi L9 array, Entropy weighted TOPSIS method, UTS.

Introduction

In a pursuit to build structural members with lower weight in automobiles and aero planes, materials like Magnesium alloys have been given due importance owing to their "higher strength to weight ratios" and good damping properties [1]. The goal is to give precise and hence trustworthy measures as required in commerce, healthcare, security, and the ecology. It's crucial in manufacturing techniques, because items must adhere to rigorous limits. The development, replication, preservation, and transmission of quantities of measuring and associated criteria should all be addressed by the material used. The accurate and lowest possible cost with prescribed specifications was made possible in micro electro mechanical (MEMS) gadgets employing the light weight magnesium alloys by completely understanding the mechanical characterestics. The formability process of the alloys is difficult and is attributed to its hexagonal lattice structure [1, 2]. Fusion welding methods of joining magnesium alloys proved to be highly unproductive due to the defects like cracks, porosity and oxides resulted in the components [3]. The process parameters not only govern the quality of weld joint but also controlnumerous aspects of microstructural evolution in TMAZ and HAZ zones [5]. AZ 91D magnesium alloys have been undergoing partial dissolution of minority phases and homogenization of microstructure with [4] loss of tensile strength [6] at elevated temperatures. With the mixing of rare earth elements like magnesium alloys,its tensile strength increases and eliminates the porosity defects. Similarly, adding modest amounts of bismuth or antimony to AZ 91 causes the precipitates of β ($Mg_{17}Al_{12}$) to refine and greatly boosts the yield strength and creep resistance at elevated temperatures [7]. Friction stir welding of AZ 61 magnesium alloys causes severe plastic deformation resulting in recrystallization of grain structure as the metal is extruded from advance side and redeposited at the retreading side [8, 9]. In the friction stir welding of AZ 31with AA 7075 by reinforcing Sic nano composites at the weld interface has caused fine microstructure due to the pinning mechanism operated at the grain boundaries [10]. The utilization of stainless-steel slag for glass-ceramics production, focusing on the impact of MgO content on Cr-spinel nanocrystal formation. The study elucidates the occurrence, distribution, and

*Corresponding author:
Tel : +91 98496 30163
E-mail: krajeshkumarphd@gmail.com

migration behavior of chromium (Cr), demonstrating that a MgO content of 12.3 wt.% enhances Cr fixation in the diopside crystal phase, resulting in glass–ceramics with high compressive strength, Vickers hardness, and minimal leaching of Cr [11]. The utilization of Friction Stir Welding (FSW) in joining Aluminum Metal Matrix Composites (AMMC), specifically AA 6063-SiC-B4C hybrid MMCs, to enhance structural performance in aerospace, automobile, and marine applications [12]. The study focuses on optimizing FSW process parameters using Taguchi L27 orthogonal array, regression analysis, and Genetic Algorithm to achieve maximum tensile strength for the hybrid composite [13].

In [14], the optimization of EDM machining settings on aluminum oxide (Al_2O_3) ceramics is achieved by combining a Taguchi-based TOPSIS technique with AHP weighting. The objectives include increased surface roughness, decreased electrode wear rate, and improved material removal rate. In order to optimize wire EDM parameters for Inconel 718 and maximize cutting speed while minimizing surface roughness and flatness error, the study [15] applies a hybrid GRA-TOPSIS algorithm with entropy weights. The lightweight design optimization of dump truck carriages is achieved in [16] by utilizing NSGA-II with entropy weighted TOPSIS in a multi-objective optimization technique that preserves structural performance. A notable mass reduction is achieved. Furthermore, research [17] examines the shear bond strength and interface quality of calcium-silicate cements and composite restorative materials, investigating variations in bond strength and crack formation under various restoration scenarios. For lightweight porous ceramics, optimize the sintering temperature in [18] to investigate features like porosity, density, compressive strength, and thermal conductivity.

The sensitivity of the solidification crack of 441 feritic stainless steel can be improved by the addition of cerium as it widens the solidification temperature range [19]; Also low additions of cerium in 434 feritic stainless steel, pitting corrosion is reduced [20]. The major contributions of this paper is follows,

- Using the FSW technique, the current research project examines the impact of cerium addition on the mechanical characteristics and microstructure of the AZ 91D magnesium alloy.
- For improving the metal peroformance, Mg AZ91D is joined by FSW processwhich eliminates traditional problems likehigh temperature during welding and consequent effects ontensile Strength andyield Strength of the magneisum alloys.

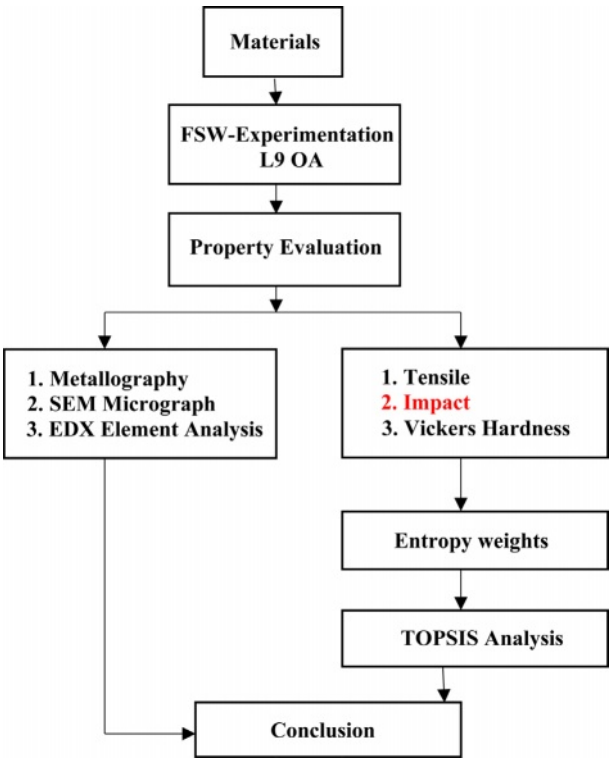

Fig. 1. Flow Chart.

Experimentation

The experimental work adopted in the investigation are illustrated in the flow chart [Fig. 1]. The mechanical properties AZ 91D Mg alloy FSW is analyzed by means of Entropy Weight Values and also the TOPSIS analysis. The jointsof the materials are analyzed for Metallography, SEM Micrograph, and EDX with element analysis. Similarly, tensile, impact and Vickers of hardness are also evaluated.

Table 1. Chemical Constituents of AZ91D Magnesium Alloy.

Material	Element % in weight							
	Mg	Al	Zn	Si	Mn	Cu	Fe	O
AZ91D	90.2	8.7	0.95	0.035	0.05	0.003	0.01	0.05

Table 2. Mechanical& Thermal Properties of AZ91D Magnesium Alloy.

Material	Ultimate Tensile strength (MPa)	Yield Strength (MPa)	% Elongation	Thermal Conductivity (W/m ^oK)	Melting Temperature (^oC)
AZ91D	230	160	3	72	533

Materials

AZ 91D Tables 1 and 2 provide the chemical composition, mechanical properties, and thermal properties of the magnesium alloys used in this investigation. The alloys are 5 mm thick plates.

The other plate is in close proximity to the grooved plate, which has a one-millimeter-deep groove filled with cerium material on its edge. Their fixation in a vice facilitates the friction stir welding procedure. The 200 μm-sized cerium particles are used to create a junction that is strengthened like an interconnected layer. Cerium is a rare earth metal and is having FCC crystal structure at room temperature.The mechanical alloying of it with magnesium alloy enhances the ductility of objects.The cerium particles are locked between the plates and hence has no scope for spillage or loss during the welding process.

Friction stir welding

As of now the magnesium alloys are preferably fabricated by employing friction stir welding method due to the advantage of joining without melting the metals. In this a tool possessing pin which goes into the metal while the shoulder portion remains on the surface and transferthe material from top to bottom and also from front to back while the shoulder generates heat and prevents the material flow astray. The tool employed for the FSW process has a pin of 5 mm diameter while shoulder is of 18 mm diameter and is heat treated to 45 HRC.

Mechanical Property Evaluation

An assessment of the joints' mechanical properties has been conducted. The impact test specimen preparation is carried out in accordance with ASTM E23 standard, as illustrated in, while the tensile test sample used is in accordance with ASTM E08 standard. The joints' microhardness was assessed using a 100 gmf force applied at 0.5 mm intervals across each joint.

In material research, project management, and control systems, monitoring and interpreting the mechanical performance is crucial. The load, and duration of loading are really the basic factors used to evaluate those mechanical characteristics. The mechanical characteristics of magnesium alloy is with the tensile strengths in the range 175-235 MPa, young's modulus in the range 44-45.5 MPa and with a poission ratio of 0.28 to 0.295.

Metallography and Scanning electron microscopy

Bakelite is used to attach the weld samples, and Sic sheets are used for polishing. The microstructure of the weld joint is captured using an Olympus optical microscope. However, this grit SiC considered as 240, 320, 400, and 600 for successive steps from 1 stage to the another. Alsoa disc grinding machine rotates at 150 rpm is mountedwith a nylon cloth and aluminium oxide particles are sprinkled over it. The samples are polishedbefore taken for metallography. The fracture evaluation is completed by using a scanning electron microscope to examine the fractured characteristics identified by the tensile test at different magnifications. While samples under the SEM were analyzed in their unetched state, samples under an optical microscope were etched using an ethanol-based picric acid solution.

(EDAX) Energy dispersive X-ray spectroscopy

It is used to determine the complex formation that takes place at the weld nugget zone using analysis of elements in the specimen's stir zone. Energy dispersive X-ray spectroscopy is based on the interaction between the sample and the X-ray excitation source, producing an emission spectrum with sets of peaks that correspond to the elements.

Design of Experiments

Statistical experimental design is more reliable and cost-effective when multiple factors are operating any system. Thus regression analysis with curve fitting method is employed to know the effect of independent variables on dependent variables. Generally speaking,

Table 4. L9 Orthogonal Array.

Run	Speed (rpm) (X1)	Feed (mm/min) (X2)	Angle (°) (X3)
1	710	16	2
2	710	20	2.5
3	710	25	3
4	900	16	2.5
5	900	20	3
6	900	25	2
7	1100	16	3
8	1100	20	2
9	1100	25	2.5

Table 3. FSW Process Parameters.

Parameters	Units	Levels		
		Low(1)	Medium(2)	High(3)
Rotational Speed (X_1)	r.p.m	710	900	1100
Weld speed (X_2)	mm/min.	16	20	25
Tool tilt Angle (X_3)	degree	2	2.5	3

curve fitting is the procedure for constructing the curve that has the best fit for the given constraints. It describes the statistical technique that used to drive for coefficient values to equations that expresses the values of one dependent variable as a function to another i.e. independent variable.The reason for choosing the curve fitting is that provides the precise data values for the given data.

A general response equation can be generated using the present investigation:

$$Y = b_0 + b_1x_1 + b_2x_2 + b_3x_3 + b_{12}x_1x_2 + b_{13}x_1x_3 + b_{23}x_2x_3 \quad (1)$$

Wherein Y is the reaction property while x_1, x_2, and x_3 are the governing variables.The evaluation of variances (ANOVA) is provided utilizing Yate's technique for the adequacy of the model fitted. The Yate's algorithm is used for computing the sum of squares and the estimated values of the results to the factorial values.

Taguchi method is also a form of Design of experiments (DOE) optimizesthe parameters while meeting the intended quality and in the current investigation L9 orthogonal array is undertaken [13, 14]. The process parameters employed with their levels have been given in Table 3 while the OA for experimentation were presented in Table 4.

TOPSIS Method

This approach computes the geometric distances between a possibility and the ideal alternative, based on the identification of weights for every criterion in the set of alternatives. Normalization is applied to the multi-character responses in order to obtain the realistic form by balancing the trade-offs between subpar and superior outcomes. This method supports for weight computation and also ensures the values mean and variance for the weight computation. For any number of inputs, we can predict the weight values for the outputs.

Entropy Weights

Entropy is a concept in information theory which measures the missing data on a random sourceandshanon entropy of the n word distribution is ($e_j=\Sigma P_{ij}\log P_{ij}$) termed as the block entropy which is a measure of the amount of information in that receiver is missing at the current state. The weights w_j for the responses are rated using entropy method by using the relation:$w_j=dj/\Sigma dj$;where $dj=1-e_j$ and j=1,2,3,….n, n=number of responses and i=1,2,….m and m=number of experiments [15]. The number of parameters and their relationship is computed for the given inputs and thus, it is used to support for any volume of data with the size N.

Results and Analysis

The experimental tests are carried out by Table 4, and they are random to remove bias and error. Table 5a displays the results of the measurement and compilation of five key variables: Vickers microhardness (H_v), Impact toughness (I_s), elongation percentage (E_l), ultimate tensile strength (UTS), and yield strength (Y_s). The yield strength has decreased while the UTS has increased as a result of the tool's higher rotating speed. The impact toughness and UTS have shown an inverse relationship as in ferrous alloys while elongation of the tensile specimen is observed to be high with low feed rates. The hardness of the joint has increased with the increase of tool angle. Larger the better criterion was used to compute the standardize decision matrix for UTS, Y_s, and I_s while the smaller the better criterion was used for E_l and H_v respectively [19] and are shown in Table 5b.

The weights of the response variables were computed from the entropies and dispersities for the overall transformation of standard decision matrix into weighted decision responses TOPSIS methodology is super imposed finally for both negative and positive ideal result by the equations (2) and (3) respectively.

Table 5. Mechanical Properties and its analysis.

Table 5a. Mechanical Properties of AZ 91D Mg alloy FSW joints with Cerium powder.

S.No	UTS(MPa)	Y_S(MPa)	I_S(Joules)	E_l (mm)	H_v
1	108.5	69.99	1.5	2	64.12
2	78.67	47.33	2	0.8	68.85
3	96.66	38.52	1.2	0.9	70.42
4	103.06	68.23	1.5	1.1	59.05
5	95.93	42.84	1.3	0.95	63.15
6	114.07	55.2	1.05	1.3	67.31
7	123.37	70.6	1	1.4	77.03
8	80.26	37.5	2.25	0.4	59.43
9	81.2	39.06	1.85	0.45	63.21

Table 5b. Standardization Decision Responses AZ 91D Mg alloy FSW joints with Cerium powder.

S.No	Standardization Decision Responses				
	UTS	Y_S	I_S	E_l	H_v
1	0.1231	0.1491	0.1099	0.0453	0.1134
2	0.0892	0.1009	0.1465	0.1133	0.1056
3	0.1096	0.0821	0.0879	0.1007	0.1032
4	0.1169	0.1454	0.1099	0.0824	0.1231
5	0.1088	0.0913	0.0952	0.0954	0.1151
6	0.1294	0.1176	0.0769	0.0697	0.1080
7	0.1399	0.1504	0.0733	0.0648	0.0944
8	0.0910	0.0799	0.1648	0.2267	0.1223
9	0.0921	0.0832	0.1355	0.2015	0.1150

Table 5c. Entropy Weighted TOPSIS Analysis of AZ 91D Mg alloy FSW joints with Cerium powder.

S.No	Weighted Decision Response(V_{ij})					Ideal solution		Coefficient of Closeness
						Positive	Negative	
	UTS	Y_S	I_S	E_l	H_v	L^+	L^-	CC
1	0.00683	0.02300	0.01883	0.02738	0.00169	0.015079	0.110237	0.879674
2	0.00495	0.01556	0.02511	0.06845	0.00158	0.030609	0.069669	0.694757
3	0.00609	0.01266	0.01507	0.06085	0.00154	0.027569	0.076108	0.73409
4	0.00649	0.02243	0.01883	0.04978	0.00184	0.014314	0.087941	0.860015
5	0.00604	0.01408	0.01632	0.05764	0.00172	0.023914	0.079376	0.768475
6	0.00718	0.01814	0.01318	0.04212	0.00161	0.016188	0.094986	0.85439
7	0.00777	0.02320	0.01256	0.03912	0.00141	0.015694	0.098432	0.862485
8	0.00505	0.01233	0.02825	0.13690	0.00183	0.098429	0.015694	0.137521
9	0.00511	0.01284	0.02323	0.12169	0.00172	0.083419	0.01859	0.182238

$$V^+=\{v^+,v^+,\ldots,v^+\}=\{(\max v_{ij}|\ j\in J\ ),\ (\min v_{ij}|\ j\in J\ )|i=1,2,\ldots,m\} \quad (2)$$

$$V^-=\{v^-,v^-,\ldots,v^-\}=\{(\min v_{ij}|\ j\in J\ ),\ (\max v_{ij}|\ j\in J\ )|i=1,2,\ldots,m\} \quad (3)$$

where, J_1&J2 are variables for Larger and smaller the better criterion respectively.

The relative distance between V_{ij} and negative and positive ideal outcomes (L^+ and L^-) are computed by utilizing equations (4) and (5)

Table 6. Mechanical Properties of AZ91D Mg alloy FSW joint without cerium powder.

Run	Parameters			(UTS)	(Ys)	(El)	(Is)	(Hv)
	Speed	Feed	Angle					
1	1100	16	3	114	71	2	1.5	103

Table 7. Regression Equation.

S.No.	Response	Regression Equation	Correlation Coefficient
1	UTS	$Y=96.263-0.263X_1-4.502X_2+0.968X_3-.017X_1X_2+5.649X_1X_3-3.089X_2X_3$	0.59
2	Y_s	$Y=50.397-0.560X_1-8.131X_2-1.028X_3-0.431X_1X_2+6.801X_1X_3-2.298X_2X_3$	0.82
3	I_s	$Y=1.394+0.042X_1+0.011X_2-0.136X_3+0.125X_1X_2-0.108X_1X_3+0.078X_2X_3$	0.6
4	E_l	$Y=1.432+0.059X_1+0.014X_2-0.136X_3+0.120X_1X_2-0.096X_1X_3+0.052X_2X_3$	0.65
5	H_v	$Y=64.358-1.118X_1+0.746X_2+2.553X_3-2.378X_1X_2+0.563X_1X_3-0.271X_2X_3$	0.54

Table 8. Analysis of Means (ANOM).

Level	X1	X2	X3
1	0.7695	0.8674	0.6239
2	0.8276	0.5336	0.5790
3	0.3941	0.5902	0.7884
Delta	0.4335	0.3338	0.2093
Rank	1	2	3

$$L^{+}_{i} = \sqrt{\sum_{i=1}^{n} (v_{ij} - v_j^{+})^2}\,,\ i = 1, 2, \ldots, m \quad (4)$$

$$L^{-}_{i} = \sqrt{\sum_{i=1}^{n} (v_{ij} - v_j^{-})^2}\,,\ i = 1, 2, \ldots, m \quad (5)$$

These distances are used to compute the closeness coefficient with respect to relative nearness of a given alternative to the positive ideal solution shown in Table 5c.

The mechanical properties of the FSW joints of the AZ 91D Mg alloy were measured for comparative evaluation (Table 6), and Table 7 displays the equations of regression for the responses. The FSW joints were also constructed without the inclusion of cerium powders at the junction. The equations of regression are implemented for each response and the adequacy of the coefficients have been tested with standard "t" statistic values. The ANOVA for each response is conducted and coefficient of correlation is evaluated.

Tables 8 and 9 display the proximity coefficients that completed the analysis of variance and analysis of means, respectively.

Discussion

The maximum strength of the FSW joint is found to be 114 MPa and it has increased to 123 MPa when cerium powder was kept between the plates before undertaking the friction stir welding process. It is attributed to the refinement of grain structure by the cerium presence during the welding process [20]. The microstructure of the base material and the welded joints with and without cerium powder applications microstructure shows that the grain size has become finer in the weld zones compared to base material, because of dynamic recrystallizations [21]. Similarly the grain dimension is also found to be fine in TMAZ and HAZ zones in the

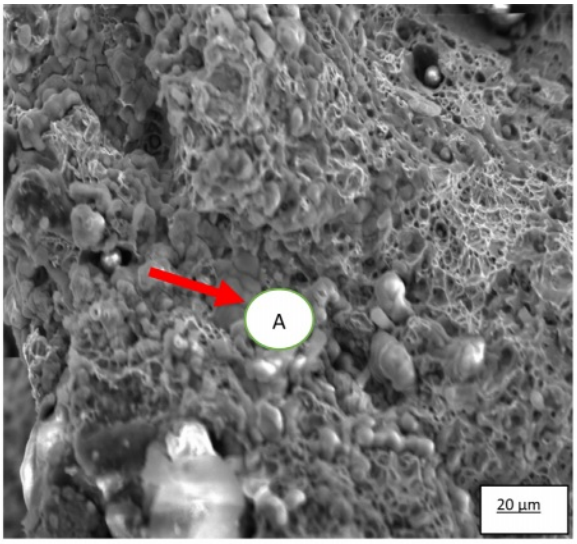

2a: SEM Micrograph

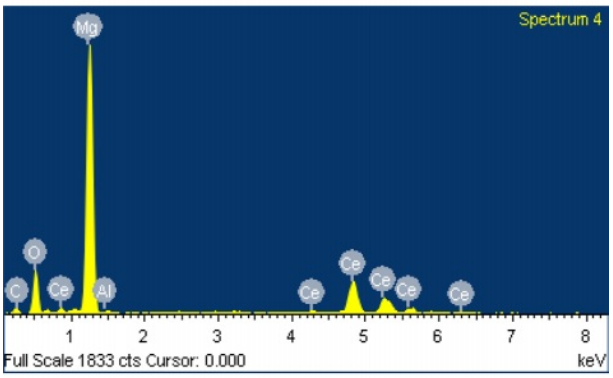

2b: EDAX survey

Fig. 2. SEM micrograph & EDAX survey.

joint produced with cerium application compared to bare welded joints. In TMAZ the metal is deformed and has shown by the upward pattern of grains without any kind of recrystallization which can be attributed to insufficient strain rate. The HAZ is affected due to weld thermal cycle only without any plastic deformation.

The SEM micrograph portrays a kind of dimple structure and cavities arisen from inclusions separated by rupture zones [Fig. 2a]. Element analysis of the fractured surface at point 'A' as shown in the micrograph is employed by the EDAX [Fig. 2b] and has been found to possesses 90% of Mg, 8% of Ce and 2% of Aluminum by

Table 9. Analysis of Variance (ANOVA).

Source	Degree of Freedom	Sum of squares	Mean Square	F	% Contribution
X1	2	0.33228	0.16614	1.36	48.4
X2	2	0.19145	0.09573	2.13	27.9
X3	2	0.07289	0.03645	0.81	10.6
Error	2	0.09000	0.04500		
Total	8	0.6863			

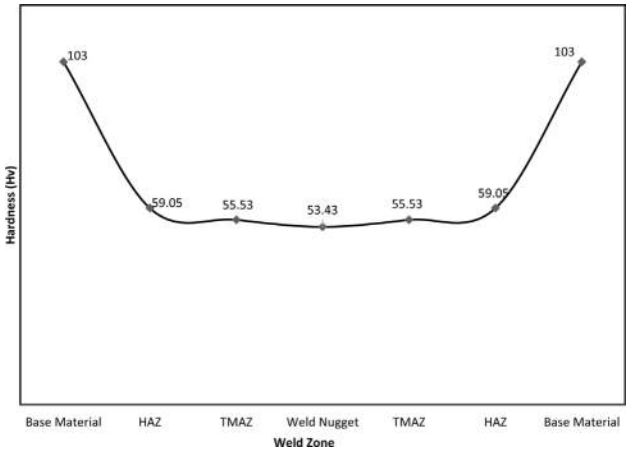

Fig. 3. Hardness survey.

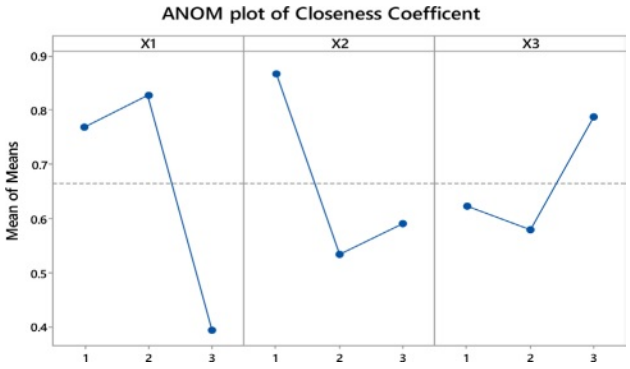

Fig. 4. Analysis of Means.

weight indicating that this location may contain $Mg_{17}Al_{12}$ and Al_4Ce_3 intermetallic compounds.The Al_4Ce_3 phase hinder grain boundary sliding reduced degree of plastic deformation and caused to improve the strength [22]. The strength of the base material is 230 MPa while the FSW joints possessed the strength in the range78-123 MPa; The reduction of it can be attributed to deflects like pinholes and cracks [Fig. 2c] with improper flow of metal coupling with insufficient consolidation of metal in the weld zone owing to low heat generation at low speeds. The elongation of the welded joint more at low feed rate than higher feed rate and can be attributed to annealing effect of the joint leading to work softening [21]. The hardness survey across the joint [Fig. 3] have shown that in the weld zones hardness is low contrasted with the neighboring TMAZ and HAZ areas owing to

Table 10. Optimal Parameters.

S. No.	Parameter	Units	Optimal Level	
			Code	Absolute value
1	X1	r.p.m	2	900
2	X2	mm/min	1	16
3	X3	degree	3	3

Table 11. Optimal responses.

Run	UTS	Y_s	E_l	I_s	H_v
1	115	70	1.95	1.75	62

the formation of Al_4Ce_3 phase [22].

The impact strength reached to a target value of 2.25J for the joint made at high rotational speed and moderate feed rates.This condition generate more heat input and there by forming coarser grain structure. The governing variables and responses are correlated by 60 to 80% and the regression equations [Table 7] so developed can be used to find the unknown responses for any given input variables.

The response plot (Fig. 4) and ANOM Analysis (Table 8) of the closeness coefficients indicate that the ideal parameters are at a mid-speed, low-feed, and high-tilt angle, as presented in Table 10. The speed of rotation govern the responses to an extent of 48.4% while the feed rate contributes to 27.9%. The tool tilt angle plays a minor role in the overall attainment of the responses. The tilt angle helps in ploughing the material from advance side and redepositing on retreating side. Thus the mode of movement of material influences, the temperature distribution and yields the microstructure accordingly [23].

The equation provides an ideal proximity coefficient of 0.881, which is the predicted value: $\mathbf{m} + \sum_{i=1}^{3} (\mathbf{mi} - \mathbf{m})$ wherein 'm' represent total mean and 'm_i' denote the median of its variable at maximal condition.

A confirmation experiment is conducted at the optimal parameters and joint is prepared. The mechanical property evaluation for the specimens drawn from this joint is performed and is given in Table 11 with a closeness coefficient of 0.862.

Conclusions

a) The responses are not unidirectional and Judgement by TOPSIS-Taguchi method in their optimization is unique and effective.
b) The response weightage by entropy method is more realistic than by any other methods.
c) Cerium powder admixture helped in refining the microstructure and eventually increased the strength.
d) At low feed rates the work softening taken place and there by the hardness is reduced in the joints.
e) At high rotational speeds more heat input is imparted and coarsening of grains taken place eventually resulted in high impact toughness.
f) Tilt angle of tool though governed less in the contribution of attainment of all responses but it caused the proper material flow eventually leading to fine microstructure.
g) Confirmation test revealed a good agreement in the results between predicted and optimal experimental

condition.

h) Hardness is computed for the developed FSW with multi-criteria decision making model. The hardness inbase material, HAZ, TMAZ and weld nugget is found to be in the descending order with a magnitude of 103,59,55 and 53 Hv respectively.

Acknowledgements

The authors thank the management of Koneru Laksmaiah Education Foundation and Vidya Jyothi Institute of Technology for the support extended during this current research work. The authors also like to thank Dr. B.V. Reddi, Department of Mechanical Engineering, V.J.I.T., Hyderabad, for giving valuable suggestions during the execution of work.

Data Availability:

The data used to support the findings of this study are available from the corresponding author upon request.

Conflicts of Interest:

The authors declare that there are no conflicts of interest pertinent to the current research paper.

Funding:

There is no funding information.

Code Availability:

There is no code availability.

Author's Contribution:

1. Vaddi venkata satyanarayana has given idea to do the work
2. Kiran kumar Dama has given the plan for execution.

References

1. M.M. Avedesian and H. Baker, ASM Int., (1999).
2. B.L. Mordike and T. Ebert, J. Mater. Sci. Eng. 30 (2001) 37-45.
3. X. Cao, M. Jahazi, J.P. Immarigeon, and W. Wallace, J. Mater. Proces. Tech. 171[2] (2006) 188-204.
4. J.A. Esparza, W.C. Davis, E.A. Trillo, and L.E. Murr, J. Mater. Sci. 21[12] (2002) 917-920.
5. L. Commin, M. Dumont, J.E. Masse, and L. Barallier, J. Acta Mater. 57[2] (2009) 326-334.
6. L. Cizek, M. Greger, L. Dobrzanski, I. Juricka, R. Kocich, L. Powlica, and T. Tanski, J. Achiv. Mater. Eng. 18[2] (2006) 203-206.
7. G. Yuan, Y. Sun, and W. Ding, J. Mater. Sci. Eng. 308 (2001) 38-44.
8. K.colligan, Weld. J. 75[7] (1999) 229-237s.
9. Kulwant Singh, G. Singh, and Harmeet Singh, J. Magnes. Alloy. 6 (2018) 292-298.
10. M. Tabasi, M. Farahani, M.K. Besharati Givi, M. Farzami, and A. Moharami, Int. J. Adv. Manufac. Tech. 86 (2016) 705-715.
11. Z. Tong, C. Xu, J. Wang, and Z. Jia, J. Ceram. Process. Res. 24[1] (2023) 17-28.
12. Gonca Deste Gökay, Rukiye Durkan, Perihan Oyar, and Gülsüm Gökçimen, J. Ceram. Process. Res. 23[1] (2022) 16-21.
13. R. Srinivasan, B. Suresh Babu, P. Prathap, Ruban Whenish, R. Soundararajan, and G. Chandramohan, J. Ceram. Process. Res. 22[1] (2021) 16-24.
14. Y.P. Zeng, CL. Lin, H.M. Dai, Y.C. Lin, and J.C. Hung, Processes 9[9] (2021) 1647.
15. P.M. Abhilash and D. Chakradhar, Process Int. Op. Sus. (2022) pp. 1-12.
16. R. Jiang, S. Ci, D. Liu, X. Cheng, and Z. Pan, Machines 9[8] (2021) 156.
17. I. Dimitrova and D. Tsanova-Tosheva, Ceramic. Process. Res. 24[2] (2023) 353-358.
18. Z. Cui, S. Xiao, X. Luo, Y. Liu, M. Liu, Y. Zeng, X. Zhong, H. Zheng, and H. Guo, Ceramic. Process. Res. 24[5] (2023) 835-840.
19. Shwangchu Zhu, Biao Yan, Metal. 9[3] (2019) 1-9.
20. Y.C. Yu, S.H. Zhang, and S.B. Wang, High Temperat. Mater. Process. 37[9-10] (2018) 807-814.
21. L. Sun, C. Miao, and L. Yang, Ecolog. Indicat. 73 (2017) 554-558.
22. Phiilip J Ross (1995) Taguchi Techniques for Quality Engineering, McGraw-Hill preferred, 2nd Edition.
23. J. Jagdesh Kumar, G. Diwakar, and V.V. Satyanarayana, Adv. Mater. Sci. Eng. (2019) 1-9.
24. Md. Muqueem, Ahemad F. Sherwani, Mukhtar Ahmad, and Zahid A. Khan, Int. J. Heavy Veh. Sys., (2009).
25. S.F. Liu, B. Li, X.H. Wang, W. Su, and H. Han, J. Mater. Process. Technol. 28[8] (2009) 3999-4004.
26. S.H.C. Park, S. Sato, and H. Kokwa, J. Mater. Sci. 38[21] (2003) 4379-4383.
27. Q. Chen, Z. Zhao, Q. Zhu, G. Wang, and K. Tao, Mater. 11[2] (2018) 250.
28. S. Ugender, J. Mag. Alloy. 6 (2018) 205-213.